JOURNAL OF GUIDANCE, CONTROL, AND DYNAMICS
Vol. 17, No. 1, January–February 1994

Targeting of Several Mars Landers

M. Lauer* and M. Hechler†
European Space Operations Centre, 64293 Darmstadt, Germany

In the baseline mission scenario considered for the Phase A feasibility study of MARSNET, three to four small surface stations are assumed to be carried to Mars on a common cruise spacecraft. During the approach to Mars this carrier spacecraft has to perform a sequence of orbit maneuvers such that the different entry probes encapsulating the surface stations can be separated on different hyperbolic orbits that enter into the Martian atmosphere at different locations. The entry locations will be chosen to reach the desired landing points on the surface of Mars, and the flight-path angle at entry typically will be restricted to values between −15 and −45 deg. In the first part of this paper conditions are derived on how to choose the landing sites on Mars. Not all latitudes can be reached for a prescribed entry flight-path angle, and the landing locations will be restricted relative to each other by the limited maneuvering capabilities of the carrier spacecraft. In the second part a feasible maneuvering sequence is constructed to deliver three surface stations to those locations required for MARSNET.

Introduction

MARSNET is one of the candidates of the next medium-size project selection in the European Space Agency (ESA) scientific program. It is considered to be embedded in a joint ESA/NASA global Mars network mission where a series of surface stations will contribute to the exploration of Mars by performing measurements in the areas of seismology, meteorology, chemistry, and geology. The ESA contribution is planned to consist of three to four station elements that are delivered to preselected landing sites, with an operational lifetime of about one Martian year. As a result of a preliminary assessment a mission concept was preferred[1,2] that can be sketched as follows.

The three surface station modules are enclosed by aeroshells (the entry probes) that are carried to Mars by the same spacecraft. The interplanetary transfer trajectory is chosen such that the first probe, after having been separated from the carrier spacecraft a few days before arrival at Mars, will reach Mars on a hyperbolic trajectory and enter into the Martian atmosphere at conditions that are required as initial conditions of an atmospheric trajectory that reaches the first of the selected landing sites on the surface. The atmospheric descent of the probe will be unguided, and about 20 km above the surface parachutes will be deployed to reduce the impact velocity on the surface to an acceptable level. After having delivered the first probe, the carrier spacecraft will execute a maneuver leading to a trajectory now targeted to the second landing site. After a period of orbit determination and correction maneuvers, the second probe will be separated from the carrier and will reach its destination. This procedure is repeated for the third and possibly a fourth probe before the carrier spacecraft is brought into an orbit around Mars or is simply targeted off to avoid an impact with the planet.

The feasibility of this multiprobe scenario depends, of course, on the feasibility of the execution of such a targeting sequence by the carrier spacecraft that delivers all surface stations to a configuration of landing sites required for the scientific objective of the mission. Or, vice versa, once the multiprobe scenario has been chosen, possible restrictions in selecting landing sites must be identified.

When constructing such a targeting sequence the following conditions have to be taken into account:

1) The entry of the probes has to be shallow enough to diminish the thermal load during descent and ensure parachute opening at a sufficient altitude. It has to be steep enough to avoid skipout and to maintain a certain landing accuracy. In the following a range from −45 to −15 deg for the entry angle is assumed to be feasible.

2) There are no means to alter the orbit of the landers after separation from the spacecraft, thus the probe will follow its orbit given by the initial conditions at separation. The effect of orbit errors present at separation due to the limited knowledge of the spacecraft state and the limited maneuvering accuracy, and the effect of errors introduced at probe separation, will be worse for long durations of this uncontrolled flight. The sequence of events just described, therefore, should not begin too early to reach a reasonable targeting accuracy at entry and thus at landing. For the same reason the time between consecutive maneuvers should be long enough to allow for orbit determination and fine corrections.

3) The last separation on the other hand cannot occur too late in the sequence because for the insertion into an elliptic orbit about Mars or for off-targeting, the carrier spacecraft will have to execute another Δv maneuver that will become increasingly more difficult the closer it gets to the entry point.

The construction of a feasible targeting sequence will be achieved in two steps. First a method is derived by which a set of landing sites and a schedule for the targeting maneuvers can be chosen, for which small velocity changes can be expected. To this purpose the relation between entry angles and landing site coordinates is discussed for the first lander separated from the carrier. Keplerian hyperbolic arcs inside the sphere of influence of Mars that satisfy the asymptotic conditions prescribed by the interplanetary trajectory are considered. It is then shown by a parametric study how a small maneuver at varying time and with varying magnitude changes the target entry point and the entry condition for a second lander separated after this maneuver. At this stage it will be possible to characterize zones on the surface of Mars that are reachable by the second lander, relative to the first, for given conditions on entry angle and maneuver capabilities. Second, the maneuvers of the carrier spacecraft requiring minimum fuel consumption are calculated for a given set of landing sites and a given time schedule of lander separations. This is done by transforming the problem into an optimization problem for a nonlinear function (the total propellant) with nonlinear constraints (the

Received July 31, 1992; presented as Paper 92-4588 at the AIAA/AAS Astrodynamics Conference, Hilton Head, SC, Aug. 10–12, 1992; revision received April 28, 1993; accepted for publication May 5, 1993.

*Visiting Scientist, Mission Analysis Section, Mission Operations Department.

†Mission Analyst, Mission Analysis Section, Mission Operations Department.

entry angle bounds), the independent variables being the arrival times at the landing sites.

Moreover, an independent section of the paper will discuss some technical details on the integration of the orbits near Mars and the computation of the entry angle level lines. In this section the regularization developed by McGehee[3] for the general, collinear, three-body problem and by Devaney[4] for mechanical systems with homogeneous potentials is extended to the restricted three-body problem as well. Navigational aspects of the problem which will influence the choice of the maneuver times of the approach targeting to a large extent will not be treated; they are the subject of Ref. 6.

Choice of the First Landing Site

As a reference, an interplanetary transfer from Earth to Mars was chosen with a launch on Feb. 1, 2001, and arrival at Mars on Oct. 25, 2001. The dates have been selected in the 2001 launch window for a DELTA 7925 launch vehicle, such that the asymptotic arrival velocity at Mars is near its minimum of about 3.8 km/s in this launch window. This is useful to obtain a minimum velocity at entry into the Martian atmosphere.

It is assumed that by slight changes in the departure conditions from Earth or by minor maneuvers made during the cruise to Mars one can change the interplanetary orbit such that the spacecraft will end up in a manifold of hyperbolic orbits (two degrees of freedom) at Mars which will have the same arrival time at the sphere of influence of Mars (radius r_s, about 577,230 km) and the same asymptotic arrival velocity. We call this manifold the arrival hyperbolas. Note that in this section we first have taken a patched conics approach; this means the hyperbolic velocity vector is generated from the interplanetary transfer conditions taking Mars as a massless point and subtracting the orbital velocity of Mars from the velocity of the arriving spacecraft. In the Mars-centered system the modulus v_∞ of this hyperbolic velocity $\boldsymbol{v}_\infty$ then defines the semimajor axis of the Mars centered hyperbola by

$$a = -\mu/v_\infty^2$$

where μ is the gravitational potential of Mars.

Some of these possible arrival hyperbolas will intersect the Martian atmosphere. At this intersection the entry location (longitude and latitude in the system rotating with Mars), the entry velocity, and the entry angle will be uniquely defined for each arrival hyperbola. The entry angle will be a quantity that is constrained, so the intention is to classify the reachable locations for a given range of entry angles.

Assume $(\boldsymbol{x}_0, \boldsymbol{v}_0)$ is an arbitrary state of the reference interplanetary trajectory inside the sphere of influence of Mars, given in the Mars-centered frame, where $\boldsymbol{x}$ and $\boldsymbol{v}$ denote the positional and the velocity part of the state. Then an entry state $(\boldsymbol{x}_e, \boldsymbol{v}_e)$ will lie on one of the arrival hyperbolas if it satisfies the following conditions:

1) The entry state $(\boldsymbol{x}_e, \boldsymbol{v}_e)$ is leading to a hyperbolic solution with respect to Mars with the same incoming asymptote velocity vector $\boldsymbol{v}_\infty$ as $(\boldsymbol{x}_0, \boldsymbol{v}_0)$.

2) The times at which the solutions through $(\boldsymbol{x}_0, \boldsymbol{v}_0)$ and $(\boldsymbol{x}_e, \boldsymbol{v}_e)$ pass the sphere of influence with radius r_s are equal.

3) The prescribed entry conditions can be written as $|\boldsymbol{x}_e| = r_e$ where $r_e = 3517.2$ km is the given radius of the outer atmosphere.

4) The angle between $\boldsymbol{v}_e$ and the tangential plane of the sphere with radius r_e at $\boldsymbol{x}_e$ is γ_e (which is the prescribed entry angle).

Any position on a hyperbolic orbit can be represented by

$$\boldsymbol{x}(t) = r\cos f\boldsymbol{u}_1 + r\sin f\boldsymbol{u}_2$$

with two orthogonal unit vectors $\boldsymbol{u}_1$ and $\boldsymbol{u}_2$, where $\boldsymbol{u}_1$ pointing to the pericenter of the hyperbola and the radius is obtained from

$$r = \frac{a(1-e^2)}{1+e\cos f} \tag{1}$$

where e is the eccentricity and f the true anomaly on the hyperbola.

We have to find two unit vectors and the three constants $a<0$, $e>1$, and t_π (epoch at pericenter) such that conditions 1–4 are fulfilled. The semimajor axis a has to be the same as it is on the reference trajectory through $(\boldsymbol{x}_0, \boldsymbol{v}_0)$ because v_∞ is the same. The eccentricity e is obtained from the definition of the entry angle

$$e = \sqrt{1+\cos^2\gamma_e(r_e/a)(r_e/a-2)}$$

The true anomalies f_s, f_e, and f_∞ at the sphere of influence, at entry, and at infinity can be found by solving Eq. (1) with r substituted by $|\boldsymbol{x}| = r_s$, r_e, ∞ and using $f_s, f_e, f_\infty \in (-\pi, -\pi/2)$. $\boldsymbol{x}_e, \boldsymbol{v}_e$ and the time t_e at which the entry point is reached can be expressed in terms of these parameters by

$$\begin{aligned}\boldsymbol{x}_e &= r_e\cos f_e\boldsymbol{u}_1 + r_e\sin f_e\boldsymbol{u}_2\\ \boldsymbol{v}_e &= (\dot r_e\cos f_e - r_e\dot f_e\sin f_e)\boldsymbol{u}_1 + (\dot r_e\sin f_e + r_e\dot f_e\cos f_e)\boldsymbol{u}_2\end{aligned} \tag{2}$$

with

$$\dot r_e = -\sqrt{|\boldsymbol{v}_e|^2 - \frac{\mu a(1-e^2)}{r_e^2}}$$

$$|\boldsymbol{v}_e|^2 = 2\mu/r_e - \mu/a$$

$$\dot f_e = \sqrt{\mu a(1-e^2)}/r_e^2$$

and

$$t_e = t_s + \Delta t$$

where t_s is the time at which the orbit through $(\boldsymbol{x}_0, \boldsymbol{v}_0)$ passes the sphere of influence first and Δt is computed from

$$\sqrt{\mu/-a^3}\,\Delta t = (e\sinh F_e - F_e) - (e\sinh F_s - F_s)$$

where F_e and F_s are the eccentric anomalies corresponding to f_e and f_s.

Finally, the two unit vectors $\boldsymbol{u}_1$ and $\boldsymbol{u}_2$ have to satisfy the equation

$$\boldsymbol{x}_\infty = \cos f_\infty\boldsymbol{u}_1 + \sin f_\infty\boldsymbol{u}_2 \tag{3}$$

where $\boldsymbol{x}_\infty$ is a unit vector in the direction of the incoming asymptote $-\boldsymbol{v}_\infty$. The set of all pairs of orthogonal unit vectors $\boldsymbol{u}_1, \boldsymbol{u}_2$ that satisfy this condition can be parameterized by the latitude of $\boldsymbol{x}_e$ as follows:

Let the longitudes and latitudes of $\boldsymbol{x}_\infty$ and $\boldsymbol{x}_e$ be denoted by $\lambda_\infty, \phi_\infty$ and λ_e, ϕ_e. Taking the scalar product of $\boldsymbol{x}_\infty$ and $\boldsymbol{x}_e$ as expressed in Eqs. (2) and (3) renders

$$\cos(\lambda_\infty - \lambda_e) = \frac{\cos(f_e - f_\infty) - \sin\phi_\infty\sin\phi_e}{\cos\phi_\infty\cos\phi_e}$$

This equation has none, one, or two solutions in λ_e modulo 2π depending on the modulus of the right-hand side being greater, equal, or less than one. The corresponding entry states are given by Eq. (2) with $\boldsymbol{u}_1$ and $\boldsymbol{u}_2$ replaced by

$$\boldsymbol{u}_1 = \frac{\cos f_e - \zeta\cos f_\infty}{1-\zeta^2}\frac{\boldsymbol{x}_0}{|\boldsymbol{x}_0|} + \frac{\cos f_\infty - \zeta\cos f_e}{1-\zeta^2}\boldsymbol{x}_\infty$$

$$\boldsymbol{u}_2 = \frac{\sin f_e - \zeta\sin f_\infty}{1-\zeta^2}\frac{\boldsymbol{x}_0}{|\boldsymbol{x}_0|} + \frac{\sin f_\infty - \zeta\sin f_e}{1-\zeta^2}\boldsymbol{x}_\infty$$

where

$$\zeta = \cos\phi_\infty \cos\phi_e \cos(\lambda_\infty - \lambda_e) + \sin\phi_\infty \sin\phi_e$$

So for a given entry angle γ_e and a given entry latitude ϕ_e the longitude at entry λ_e is determined, which almost provides the curves of constant entry angle we seek.

One refinement still has to be made at this point. The entry angle γ_e^{rot} required for the aerodynamic calculations inside the Martian atmosphere is given relative to the system rotating with the atmosphere. This is slightly different from the angle γ_e defined by the inertial state vector in the fourth condition just given. To obtain the states which satisfy conditions 1-3 with given entry angle γ_e^{rot} instead of condition 4, the same calculations together with a suitable iteration method are used.

Curves of constant entry angle γ_e^{rot} in terms of latitudes and longitudes in the rotating Mars system are shown in Fig. 1. These are obtained from ϕ_e and λ_e, which refer to a nonrotating coordinate system, by considering the rotation angle of Mars at the time of entry t_e.

For entry angles between -15 and -30 deg landing sites at latitudes between -71 and $+80$ deg can be reached, assuming only one lander is delivered to Mars. Reachable longitudes can be assumed not to be restricted because the arrival time can be easily changed by changing the launch conditions or by a maneuver made early on during the cruise to Mars.

Before going into the discussion on how to deliver more than one lander we have to make an excursion into the methods used, because from now on we will handle the problem more precisely than we can with patched conics.

Orbit Integration Near Mars

The governing equations for the motion of a small spacecraft in the (nonrotating) Mars-centered, mean-Earth equatorial system of 1950.0 (MEE1950) are

$$\dot{x} = v \qquad \dot{v} = -\frac{Gm_M}{|x|^3}x - \sum_j Gm_j\left\{\frac{d_j}{|d_j|^3} - \frac{d_j - x}{|d_j - x|^3}\right\}$$

where the sum includes all relevant masses and G = the gravitational constant, m_M = Mars' mass, m_j = the mass of body j, d_j = the position vector of mass j in the MEE1950 system, and x = position vector of the spacecraft in the MEE1950 system.

As an approximation only the term in the sum that corresponds to the sun is considered and the position vector of the sun d_s is assumed to move on the circle:

$$d_s = WR\begin{pmatrix}\cos\omega t\\ \sin\omega t\\ 0\end{pmatrix}$$

with an orthogonal matrix W and real numbers ω and R.

W is computed such that the circle lies in the plane spanned by the position and velocity vector of the sun relative to Mars at time $t = 0$, that is the time at which the initial values are given. The norm of the position vector determines R. The ω is evaluated from the relation

$$\omega^2 R^3 = G(m_S + m_M)$$

which is required to let the approximated motion of the sun with mass m_S around Mars satisfy Newton's law.

With this approximation the differential equations are those of the restricted three-body problem, and several transformations are applied to put these equations into the standard form. The transformation

$$x' = W^t x \qquad v' = W^t v$$

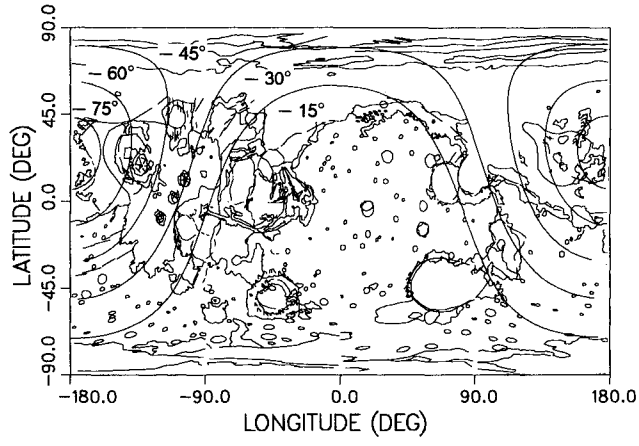

Fig. 1 Accessible landing sites with corresponding entry angles.

gives coordinates in the plane of the circular motion of d_s. The transformation

$$x' = (1-\mu_M)R\begin{pmatrix}\cos\omega t\\ \sin\omega t\\ 0\end{pmatrix} - x$$

$$v' = (1-\mu_M)R\omega\begin{pmatrix}-\sin\omega t\\ \cos\omega t\\ 0\end{pmatrix} - v$$

$$\mu_M = \frac{m_M}{m_M + m_{\text{sun}}}$$

gives coordinates with respect to the mass center of the sun and Mars.

Scaled coordinates are introduced by:

$$s = \omega t, \qquad q = \frac{x}{R}, \qquad p = \frac{v}{R\omega}$$

The transformation

$$q' = \begin{pmatrix}\cos s & \sin s & 0\\ -\sin s & \cos s & 0\\ 0 & 0 & 1\end{pmatrix}q$$

$$p' = \begin{pmatrix}-\sin s & -\cos s & 0\\ \cos s & -\sin s & 0\\ 0 & 0 & 1\end{pmatrix}q + \begin{pmatrix}\cos s & \sin s & 0\\ -\sin s & \cos s & 0\\ 0 & 0 & 1\end{pmatrix}p$$

gives coordinates in a system rotating uniformly around the center of mass.

As the orbits are very near the primary at $(1-\mu_M)e_1$, with $e_1 = (1,0,0)^T$, regularizing coordinates are used by the following two transformations. This technique, which removes the singularity, was derived from the one originally given by McGehee[3] for the general, collinear, three-body problem.

The transformation

$$q' = q \qquad p' = \sqrt{\rho}\,p \qquad \rho = |q - (1-\mu_M)e_1|$$

and time transformation

$$\mathrm{d}s = \rho^{3/2}\,\mathrm{d}\tau$$

lead to the final form of the equations:

$$q = \rho p$$

$$\dot{p}_1 = \frac{q_1-(1-\mu_M)}{2\rho} p_1^2 + \frac{q_2}{2\rho} p_1 p_2 + \frac{q_3}{2\rho} p_1 p_3 + \rho^2 q_1 + 2\rho^{3/2} p_2 - \mu_M \frac{q_1-(1-\mu)}{\rho} - (1-\mu_M)\frac{q_1+\mu_M}{\sigma^3}\rho^2$$

$$\dot{p}_2 = \frac{q_1-(1-\mu_M)}{2\rho} p_1 p_2 + \frac{q_2}{2\rho} p_2^2 + \frac{q_3}{2\rho} p_2 p_3 + \rho^2 q_2 - 2\rho^{3/2} p_1 - \mu_M \frac{q_2}{\rho} - (1-\mu_M)\frac{q_2}{\sigma^3}\rho^2$$

$$\dot{p}_3 = \frac{q_1-(1-\mu_M)}{2\rho} p_1 p_3 + \frac{q_2}{2\rho} p_2 p_3 + \frac{q_3}{2\rho} p_3^2 - \mu_M \frac{q_3}{\rho} - (1-\mu_M)\frac{q_3}{\sigma^3}\rho^2$$

The differential equations are integrated numerically using a Runge-Kutta method of order 7/8 with variable step size. It turns out that the step size is usually chosen such that about 20 steps are needed for a travel time of one day along the approaching orbit.

In connection with the preceding orbit integration, in the following section we will investigate the effect on the entry angle by a maneuver performed Δt days before arrival. A maneuver is defined by its size Δv and its direction which can be stated as longitude and latitude (λ, ϕ) on a unit sphere. We will generate level lines on this unit sphere each point of which, after propagation along the approach orbit, will reach the entry altitude at the same prescribed entry angle γ_e.

Numerically this is done by a continuation method. We define a vector field of unit length which has orbits in the level lines of γ_e by

$$X(\lambda, \phi) = \frac{1}{\left|\left(\frac{\partial\gamma_e}{\partial\lambda}, \frac{\partial\gamma_e}{\partial\phi}\right)\right|} \begin{pmatrix} \frac{\partial\gamma_e}{\partial\phi} \\ -\frac{\partial\gamma_e}{\partial\lambda} \end{pmatrix}$$

The partial derivatives are approximated by the finite differences:

$$\frac{\partial\gamma_e}{\partial\lambda}(\lambda, \phi) = \frac{\gamma_e(\lambda+\Delta\lambda, \phi)-\gamma_e(\lambda, \phi)}{\Delta\lambda}$$

$$\frac{\partial\gamma_e}{\partial\phi}(\lambda, \phi) = \frac{\gamma_e(\lambda, \phi+\Delta\phi)-\gamma_e(\lambda, \phi)}{\Delta\phi}$$

The level line through a point (λ_0, ϕ_0) can now be computed by integration of the vector field using a Runge-Kutta method of order four. Care has to be taken when the level line is not connected, because a single integration can give only one connected component of the level line. In this case two initial values (λ_0, ϕ_0) have to be integrated.

General Effect of Maneuvers on Approach Trajectory

The interplanetary orbit was adjusted to aim at an entry point at $\lambda = -74$ deg, $\phi = 24$ deg which is a reference point, chosen near a desired landing site at Lunae Planum. So the first lander can reach this point by separation from the spacecraft at any time on the orbit of the spacecraft near Mars.

To get a general view of the effect of maneuvers at various times and of various magnitudes on the approaching orbit the reference state is integrated backward from entry over a time interval Δt. Then maneuvers are applied by changing the velocity part of the state vector. This is done with a fixed amount Δv in varying directions. The resulting states are again integrated forward until they reach the entry height above Mars.

As the arrival velocity of the spacecraft relative to Mars is about 3.8 km/s the interplanetary orbit enters the sphere of influence about two days before atmospheric entry. To see how the entry angle and the entry point vary with the direction of the maneuver, Δt and Δv fixed, lines of constant entry angle are computed on a sphere (called the velocity sphere) represented by longitude and latitude of the direction of the applied maneuver given in the mean-Earth equatorial system of 1950.0. The method of generating these level lines has been described in the preceding section. These lines are then integrated forward until they reach the entry height, and the longitude and latitude of the corresponding points above the surface of Mars (on the entry sphere) are plotted.

The landing points can then be computed by applying an atmospheric entry trajectory integrator using the characteristics of the Mars' surface and atmosphere and of the parachute deployments (for details see Ref. 5). This has been done for one of the level lines until deployment of the first parachute, which usually takes place at a height of less than 20 km above the Mars' reference ellipsoid. The actual landing points differ by less than 1 deg in longitude and latitude from the points of parachute deployment. The computations show that over the atmospheric trajectory from entry to the surface the lines of equal entry angle are shifted some 5 deg eastward in longitude.

The mapping of the constant entry angle lines on the velocity sphere to the entry sphere for maneuvers (free direction) six days before entry with $\Delta v = 5$ m/s is illustrated by Figs. 2 and 3.

Only velocity changes in a direction lying on a kind of hemisphere lead to trajectories that reach Mars. Velocity changes in the opposite direction will raise the pericenter height above the entry altitude. We call the map that associates a point on the

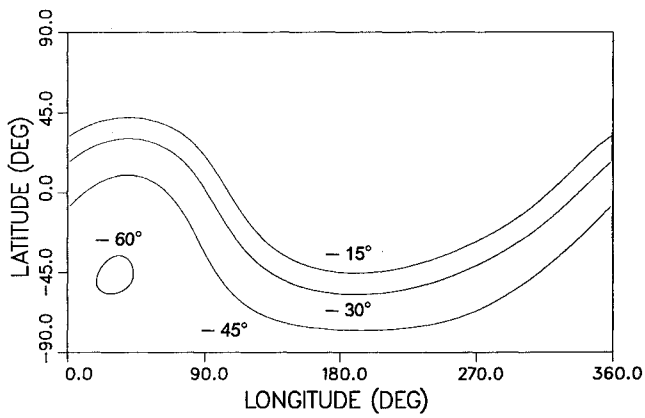

Fig. 2 Entry angle level lines—six days before entry, 5 m/s.

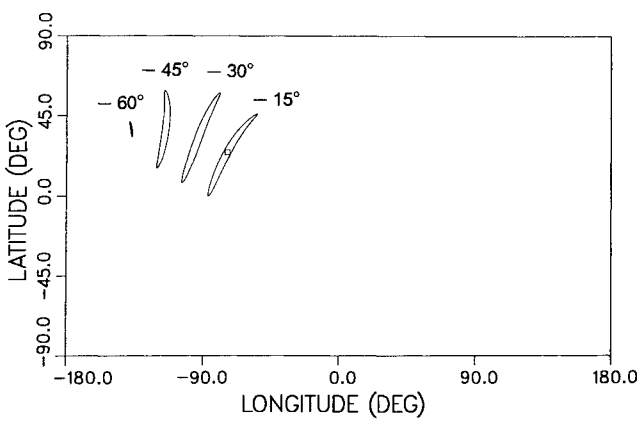

Fig. 3 Mapped entry angle level lines—six days before entry, 5 m/s.

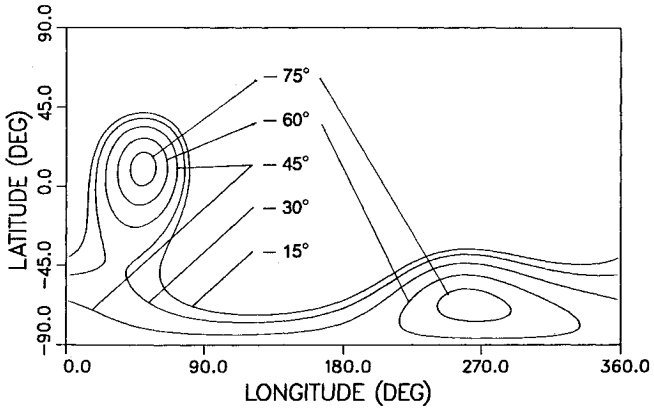

Fig. 4 Entry angle level lines—six days before entry, 20 m/s.

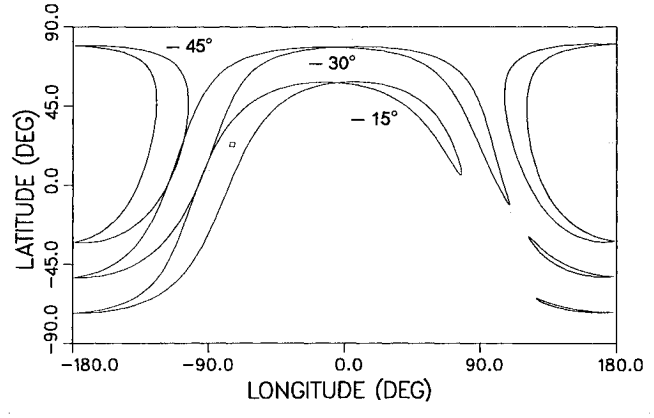

Fig. 5 Mapped entry angle level lines—six days before entry, 20 m/s.

velocity sphere with a point on the entry sphere, when the respective trajectory meets the Mars' atmosphere, the target map. The aforementioned area on the velocity sphere becomes its domain. The entry angle is a smooth function on this domain that vanishes when approaching the boundary and takes its minimum of about -61 deg at a point near $\lambda = 30$ deg, $\phi = -50$ deg (for the given Δv and Δt). The level lines are all connected and of circle-like shape. The image of these lines under the target map shown in Fig. 3 indicates that the entire domain of the target map is mapped onto a set of points having longitudes between -140 and -30 deg and latitudes between 0–60 deg. Most of the points in this image may originate from two points on the velocity sphere. In other words, for a given entry point there may be two solutions with the same Δv modulus but different entry angles; the map is not one-to-one.

If we increase the maneuver size to $\Delta v = 10$ m/s the domain of the target map becomes a slightly distorted hemisphere and the level lines become distorted circles. The image of the domain on the entry sphere is extended, now covering a greater area.

For $\Delta v = 20$ m/s (see Figs. 4 and 5) the entry angle shows two minima on the velocity sphere, one of -89 deg at $\lambda = 50$ deg, $\phi = 0$ deg and one of -85 deg at $\lambda = 260$ deg, $\phi = -70$ deg. The level lines for values less than -45 deg are no longer connected but consist of two circles around each of the minima. The domain of the target map is further decreasing whereas its image is increasing, now covering a greater part of the entry sphere, but still leaving a great part uncovered. A significant region eastward and southward of the reference point near Lunae Planum is still unreachable.

For $\Delta v = 50$ m/s the domain breaks up into two small disks around the points $\lambda = 244$ deg, $\phi = -51$ deg and $\lambda = 54$ deg, $\phi = 28$ deg; these points are near the direction of Mars ($\lambda = 239$ deg, $\phi = -40$ deg) or opposite to it ($\lambda = 59$ deg, $\phi = 40$ deg). Just the same development of the domain and the image of the entry map appear to take place when Δt is varied, rather than Δv. In fact, one can derive the rule of thumb that maneuvers with

$$\Delta t \times \Delta v = \text{const} \tag{4}$$

have nearly the same effect. Table 1 shows the maximum distance (km) on the surface from the Lunae Planum point which can be reached on the -15 deg and the -30 deg level lines, respectively, for several combinations of Δv and Δt. The first column gives the time before arrival (days), the second the maneuver Δv (m/s), the third the product of both (km).

Table 1 Maximum deviation on level lines from target point

Δt, days	Δv, m/s	$\Delta t \times \Delta v$, km	-15 deg level line	-30 deg level line
1	10	864	564	1259
1	15	1296	848	1433
1	20	1728	1132	1643
2	10	1728	1115	1633
6	5	2592	1668	2089
5	7	3024	1949	2358
1	35	3024	2001	2406
3	12	3110	2016	2425
4	10	3456	2239	2640
6	10	5184	3426	3821
10	10	8640	6250	6793

The result shows that the constant in the preceding rule of thumb can be identified with this maximum distance, defined by the extreme points of the mapped level line pattern. Further, some similarity between the pattern in Fig. 5 and that in Fig. 1 can be observed. This indicates that retargeting of the second probe relative to the first during the Mars' approach is related to moving the first entry point while keeping the arrival time constant, as has been discussed in the second section of this paper. In both cases the components orthogonal to the trajectory will affect the motion of the entry point. The preceding rule of thumb together with Fig. 1 allows a preliminary assessment of the possibility of reaching a desired configuration of landing points on the surface of Mars for given entry angle and maneuver constraints.

Optimal Maneuver Sequence

Once a triple of three landing sites and a schedule for the lander separations are chosen one has to construct an initial approach orbit and two maneuvers such that:

1) The three landers, which are separated from the spacecraft before the maneuvers and after the first and the second one, reach the given landing sites.

2) The flight path angles of the landers at entry are in a suitable range.

Among various possibilities those with minimal total Δv are preferable. The solution will depend on several parameters: the three landing sites represented by their longitude λ and latitude ϕ and the sequence in which they shall be reached, the interval $(\gamma_{\min}, \gamma_{\max})$ which is allowed for the three entry angles, the time Δt_1 of the first maneuver measured from the time of entry of the arrival orbit, and the time Δt_{man} between the two maneuvers.

As described before, an arrival orbit and the initial arrival time T_e^1 are fixed by the first landing site and the corresponding entry angle γ_1. The state vector at the time of the first maneuver $T_m^1 = T_e^1 - \Delta t_1$ in the MEE system is therefore given and shall be denoted by (x_0, v_0). A maneuver sequence, which satisfies the first of these two conditions, is found from the solutions of the two boundary value problems (BVP).

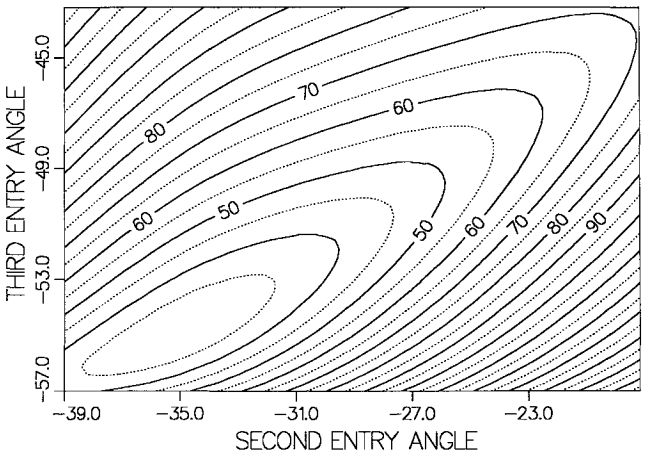

Fig. 6 Contour lines of total Δv of maneuver sequence.

Problem 1:

$$\dot{x} = v \qquad \dot{v} = -\frac{Gm_M}{|x|^3}x - F_1(x, t)$$

$$x(0) = x_0 \qquad x(s_1) = x_2(s_1)$$

Problem 2:

$$\dot{x}' = v' \qquad \dot{v}' = -\frac{Gm_M}{|x'|^3}x' - F_2(x, t)$$

$$x'(0) = x(\Delta t_{\text{man}}) \qquad x'(s_2) = x_3(s_2)$$

which satisfy

$$|x(u)| > R_e, \qquad 0 \le u < s_1 \tag{5}$$

$$|x'(u)| > R_e, \qquad 0 \le u < s_2 \tag{6}$$

where R_e is the radius of the entry sphere, t is measured from T_m^1 in the first case and from $T_m^2 + \Delta t_{\text{man}}$ in the second case, $F_i(x, t)$ are the perturbing forces as derived before, $x_2(s_1)$ is the position of the second landing site in the MEE system at the time $T_e^1 = T_m^1 + s_1$ called the second target point, $x_3(s_2)$ is the position of the third landing site in the MEE system at the time $T_e^2 = T_m^1 + s_2 + \Delta t_{\text{man}}$ called the third target point, and s_1, s_2 are arbitrary.

The Δv required for the first maneuver is then

$$\Delta v_1 = v(0) - v_0$$

and for the second maneuver

$$\Delta v_2 = v'(0) - v(\Delta t_{\text{man}})$$

For the case of vanishing perturbations these boundary value problems become Lambert problems which have exactly two hyperbolic solutions, one corresponding to a transfer angle between 0 and π and the other corresponding to a transfer angle between π and 2π.

Every hyperbola has two intersections with the entry sphere, if it has any, and if the exceptional case of the intersection at pericenter is excluded. Corresponding to the order in which they are reached on the orbit they are called entry and exit. In the case of a transfer angle greater than π the target point is always the exit such that the orbit has an arc inside the entry sphere and so violates Eq. (5) or Eq. (6). In the case of a transfer angle between 0 and π the target point can be entry or exit. The BVP's together with the conditions (5) and (6) have therefore one or no solution in the case of vanishing perturbations depending on the position of the targets.

Solutions for the perturbed case are now found by a shooting method with the solution of the Lambert problem as the starting value. Conditions (5) and (6) have to be verified for the resulting orbits but it turns out that in most cases they are satisfied if these conditions are fulfilled by the Lambert solutions.

In the preceding formulation the two arrival times T_e^2 and T_e^3 can still be freely chosen. This means we can now generate a maneuver sequence that satisfies the condition necessary to reach the prescribed entry points and present the resulting $\Delta v_i = |\Delta v_i|$ and the entry angles γ_2 and γ_3 as functions of these times. The problem is thus reduced to finding suitable values of T_e^2 and T_e^3 such that the entry angle condition is met and $\Delta v_1 + \Delta v_2$ is minimal. This is an optimization problem for the nonlinear objective function

$$\Delta v_1(T_e^2, T_e^3) + \Delta v_2(T_e^2, T_e^3)$$

with the nonlinear constraints

$$-45 \text{ deg} \le \gamma_2(T_e^2, T_e^3) \le -15 \text{ deg}$$

and

$$-45 \text{ deg} \le \gamma_3(T_e^2, T_e^3) \le -15 \text{ deg}$$

A standard numerical optimization routine was used to solve this problem. But rather than presenting the formal result of this optimization we proceed to discuss the behavior of the objective function.

It is possible to transform the independent variables from arrival times to entry angles (in the rotating frame), at least locally. The constraints then become linear functions of the independent variables and the minima can be easily read off from contour lines of the performance function. This transformation is allowed because for a locally fixed entry location there is a one-to-one relation of entry angle and arrival time.

In the following computations the three landing sites $\lambda = -70$ deg, $\phi = -45$ deg; $\lambda = -65$ deg, $\phi = 20$ deg; and $\lambda = -120$ deg, $\phi = -15$ deg were chosen following the updated recommendations in Ref. 2. The reference orbit arrives on 18925.27041 (Modified Julian Day 1950) at the first site with the entry angle $\gamma_1 = -15$ deg. The first maneuver takes place five days before entry and the second one two days after the first one. Figure 6 shows the contour lines of the sum of the various Δv as a function of the entry angles at the second and third entry points.

The minimum of Δv is at $\simeq 33$ m/s for $\gamma_2 \simeq -35$ deg and $\gamma_3 \simeq -55$ deg. The entry angles at the minimum are those expected from the initially discussed no-change-of-arrival-time approximation. $\gamma_3 = -55$ deg is outside the admissible interval (notice that the transformation to the rotating frame has been done). This means that to reach $\gamma_3 > -45$ deg a penalty in Δv will have to be accepted.

One possible way of satisfying the entry angle constraint at the third entry point would be to merely modify the second maneuver such that the arrival time T_e^3 is delayed. Figure 6 shows that this would result in a total Δv of $\simeq 100$ m/s. A better possibility, however, is to modify both maneuvers by also delaying the second arrival time T_e^2. The second entry angle then becomes $\gamma_2 \simeq -21$ deg and the total Δv is only 65 m/s. Clearly it is cheaper to change the arrival time if this change takes place earlier before entry.

Parametric studies have been performed changing the maneuver times. The following minimum total Δv have been obtained for $-45 \text{ deg} \le \gamma_i \le -15$ deg: $\simeq 60$ m/s if the second maneuver takes place one day instead of two days after the first one, $\simeq 45$ m/s if the maneuvers take place seven and five days before entry, and $\simeq 175$ m/s if the maneuvers take place two and one days before entry.

For a sequence of four targets consisting of a modification of the original triple and an additional point on the opposite

side of Mars only 44 m/s total Δv is required. In that case the maneuvers take place 10, 4, and 2 days before entry.

Conclusions

The targeting of several landers to the surface of Mars using one common carrier spacecraft that does all orbit maneuvering and separates the entry probes one after the other during the last 10 days of the approach toward Mars is feasible within an acceptable propellant budget and allowing the delivery of the surface stations to places of scientific interest, e.g., a triangle around the Tharsis area can be reached. In this multiprobe scenario restrictions on the choice of landing sites relative to each other are imposed because the range of acceptable entry angles is constrained by the design limitations of the atmospheric probes and the atmospheric trajectories that can be flown.

Calculations of the retargeting maneuver effects using rather precise trajectory models confirm the approximate results that can be presented using Keplerian motion with fixed arrival time only. The landing points have to be chosen within the bands between the entry angle limits as shown in Fig. 1. This pattern of reachable zones can be shifted East-West by changing the arrival time of the carrier, so it is mainly a restriction on the relative locations. An approximation of the maneuver sizes is given by formula (4).

Minimum total Δv maneuver sequences have been constructed for a given set of three or four landing points, and prescribed times of maneuver execution. Three probes can be delivered with 65 m/s starting five days before arrival. Four probes including one on the opposite side of Mars relative to the other three can be delivered using 44 m/s. The penalties that are introduced if the optimum values of the entry angles cannot be acquired have also been discussed.

Acknowledgment

M. Lauer gratefully acknowledges the support of a European Space Agency fellowship.

References

[1]"Mission to Mars," Rept. of the Mars Exploration Study Team, ESA SP-1117, July 1989.

[2]"MARSNET, A Network of Stations on the Surface of Mars," Rept. on the Assessment Study, ESA SCI(91)6, Jan. 1991.

[3]McGehee, R., "Triple Collision in the Collinear Three-Body Problem," *Inventiones Mathematicae,* Vol. 27, 1974, pp. 191–227.

[4]Devaney, R. L., "Singularities in Classical Mechanical Systems," *Ergodic Theory and Dynamical Systems,* Birkhauser, Boston, MA, 1981.

[5]Hechler, M., and Gonzalez-Laguna, E., "MARSNET-ISABELLA Assessment Study Mission Analysis," ESA-ESOC-MAS Working Paper 310, Aug. 1990.

[6]Hechler, M., and Lauer, M., "MARSNET—Phase A Mission Analysis: Navigation," AIAA/AAS Astrodynamics Conference, AIAA Paper 92-4587, Hilton Head, SC, Aug. 1992.